ЖУРНАЛ СТРУКТУРНОЙ ХИМИИ

2012. Том 53, № 3 *Май – июнь* *С. 540 – 547*

UDC 548.737:547.23

MOLECULAR STRUCTURE, QUANTUM CHEMICAL INVESTIGATION, AND THERMAL BEHAVIOR OF $(DNAZ\text{-}CO)_2$

H.X. Ma[1], N.N. Zhao[1], B. Yan[1,2], Y.L. Guan[1], J.F. Li[1], J.R. Song[1,3]

[1]*College of Chemical Engineering, Shaanxi Key Laboratory of Physico-Inorganic Chemistry, Northwest University, X i'an, Shaanxi, P. R. China,* e-mail: mahx@nwu.edu.cn
[2]*School of Chemistry and Chemical Engineering, Yulin University, Yulin, Shaanxi, P. R. China*
[3]*Conservation Technology Department, the Palace Museum, Beijing, P. R. China*

Received December, 14, 2010

Bis-(3,3-dinitroazetidinyl)-oxamide ($(DNAZ\text{-}CO)_2$) is an acyl derivative of 3,3-dinitroazetidine (DNAZ). It is prepared and its crystal structure is determined. The crystal is orthorhombic, *Fdd*2 space group, $a = 13.136(14)$ Å, $b = 19.48(3)$ Å, $c = 10.326(14)$ Å, $V = 2642$ (6) Å^3, $Z = 8$. A density functional theory (DFT) method of the Amsterdam Density Functional (ADF) package is used to calculate the geometry, frequencies, and properties. The optimized geometry, frontier orbital energy, and main atomic orbital percentage are obtained. The thermal behavior is studied under a non-isothermal condition by DSC and TG/DTG methods. The apparent activation energy (E_a) and pre-exponential factor (A) of the exothermic decomposition reaction of $(DNAZ\text{-}CO)_2$ are 164.10 kJ·mol^{-1} and $10^{13.38}$ s^{-1} respectively. The critical temperature of thermal explosion is 272.20 °C. The values of $\Delta S^{\neq}$, $\Delta H^{\neq}$, and $\Delta G^{\neq}$of this reaction are 6.44 J·mol^{-1}··K^{-1}, 163.76 kJ·mol^{-1} and 160.34 kJ·mol^{-1} respectively.

K e y w o r d s: bis-(3,3-dinitroazetidinyl)-oxamide ($(DNAZ\text{-}CO)_2$), molecular structure, quantum chemical investigation, thermal behavior.

INTRODUCTION

Dinitro- and trinitro-derivatives of azetidine are of interest because they contain a strained ring system. This makes them good candidates for energetic materials (propellants or explosives). Initial reports concentrated on the synthesis of 1,3,3-trinitroazetidine (TNAZ), including the synthesis of 3,3-dinitroazetidine (DNAZ) [1, 2]. As one of the important derivates of TNAZ, DNAZ [2, 3] can provide a variety of solid energetic materials with high oxygen balance [3—12]. In this paper, an acyl derivate of DNAZ, bis-(3,3-dinitroazetidinyl)-oxamide ($(DNAZ\text{-}CO)_2$) was synthesized, and a single crystal suitable for the X-ray measurement was obtained. The Amsterdam Density Functional (ADF) [13—15] program was used to calculate the geometry, frequencies, and properties. Therefore the optimized geometry, frontier orbital energy, and main atomic orbital percentage were obtained so as to deepen the study of the structure-properties relationship of this material. The thermal behavior was studied by DSC and TG/DTG techniques and the non-isothermal kinetics parameters were determined by means of Kissinger and Ozawa methods.

EXPERIMENTAL

Materials. DNAZ was prepared and purified by a reported method [2]. Other chemicals and reagents used in the synthesis of $(DNAZ\text{-}CO)_2$ were analytically pure and used without further purification.

Table 1

Crystallographic data and structure determination details for $(DNAZ\text{-}CO)_2$

Empirical formula	$C_8H_8N_6O_{10}$
CCDC deposition number	782,444
Formula mass, $g \cdot mol^{-1}$	348.20
Temperature, K	296(2)
Crystal dimension, mm	0.29×0.21×0.15
Crystal system	Orthorhombic
Space group	*Fdd*2
a, *b*, *c*, Å	13.146(14), 19.48(3), 10.326(14)
V, Å^3	2642 (6)
Z	8
D_c, $g \cdot cm^{-3}$	1.751
μ, mm^{-1}	0.163
F(000)	1424
θ ranges, deg.	2.72—25.07
h, *k*, *l*	–15—15, –23—11, –12—11
Reflections collected	3112
Independent reflections (R_{int})	1155 (0.0493)
Data / restraints / paramenters	1975 / 1 / 110
Goodness-of-fit on F^2	1.040
Final R_1, wR_2 [$I > 2\sigma(I)$][a]	0.0439, 0.1024
R_1, wR_2 indices (all data)[a]	0.0579, 0.1024
Largest difference peak and hole, eÅ^{-3}	0.158, –0.141

[a] $w = 1/[\sigma^2(F_0^2) + (0.0607P)^2]$, where $P = (F_0^2 + 2F_c^2)/3$.

Physical measurements. Elemental analysis was performed on a PE-2400 (Perkin-Elmer, USA) elemental analyzer. The FT—IR spectra were recorded using KBr discs (4000—400 cm^{-1}) on a Nicolet 60 SXR (Nicolet, USA) FT—IR spectrophotometer. The ^1H NMR and ^{13}C NMR spectra in CD_3COCD_3 were obtained using an INOVA-400 NMR (VARIAN, USA) spectrometer.

Preparation of $(DNAZ\text{-}CO)_2$. $(DNAZ\text{-}CO)_2$ used in this work was prepared according to the following method. A solution of DNAZ (0.47 g, 3.2 mmol), oxalyl chloride (0.18 ml, 2.0 mmol), and $NaHCO_3$ (0.28 g, 3.2 mmol) in dichloromethane (30.0 ml) was stirred under reflux for 5 h. The reaction mixture was concentrated in vacuo, acetone (50 ml) was added, and the mixture was stirred for 30 min, settled, and filtered. The solid product was washed with ethanol and purified by recrystallization from dichloromethane to give the pure colorless compound with 78.6 % yield. A single crystal suitable for the X-ray measurement was obtained by slow evaporation in dichloromethane for 7 days. Anal. Calc. (%) for $C_8H_8N_6O_{10}$: C, 27.60; N, 24.14; H, 2.316. Found (%): C, 27.41; N, 24.04; H 2.302; IR (KBr, cm^{-1}): 2966.88, 2899.14, 1648.85, 1572.78, 1365.31; ^1H NMR(CD_3COCD_3): 5.526(s, 4H), 5.045(s, 4H); ^{13}C NMR(CD_3COCD_3): 58.323(C-1,3), 108.384(C-2), 158.946(C=O).

X-ray crystallography. Diffraction data were collected at room temperature on a Bruker SMART APEX CCD X-ray diffractometer (Bruker, Germany) with MoK_α radiation (λ = 0.71073 Å) using the ω scan mode. Unit cell dimensions were obtained with least-squares refinements, and semi-empirical absorption corrections were applied using the SADABS program [16]. The structure was solved by direct methods and refined by full-matrix least squares techniques based on F^2 with the SHELXTL-97 program [17]. All non-hydrogen atoms were obtained from the difference Fourier map and refined with atomic anisotropic thermal parameters. The hydrogen atoms were added according to the theoretical models. The details of data collection and refinement are given in Table 1.

CCDC-782444 contains the supplementary crystallographic data for the title compound. The data can be obtained free of charge at www.ccdc.cam.ac.uk/conts/retrieving.html or from the Cambridge Crystallographic Data Centre (CCDC), 12 Union Road, Cambridge CB2 1EZ, UK; fax: +44(0)1223 –336033; e-mail: deposit@ccdc.cam.ac.uk.

Quantum chemical calculations. Single crystal structural data for the title compound were used in the theoretical calculations. The DFT calculation was performed using the ADF 2005.01 package [13—15]. The local density approximation (LDA) characterized by the Vosko—Wilk—Nusair (VWN) parameterization has been adopted for the geometry optimization [18]. The PW91 generalized gradient approximation (GGA) exchange-correlation functional has been used for the energy calculation [19, 20]. Large Slater-type orbital (STO) basis sets (triple-ζ) without frozen core approximation were employed as basis functions to describe the atomic orbitals on each atom. Integrals were numerically calculated with an accuracy of six digits. In addition, a frequency calculation was performed to check if the stationary point was the potential minimum and obtain thermodynamic properties.

Thermal decomposition conditions. The DSC and TG-DTG experiments for $(DNAZ\text{-}CO)_2$ were performed using a model Q600SDT (TA, USA) under a nitrogen atmosphere, at a flow rate of 100 $ml \cdot min^{-1}$ with the sample mass of about 1.030 mg. The heating rates used were 2.5 $°C \cdot min^{-1}$, 5.0 $°C \cdot min^{-1}$, 10.0 $°C \cdot min^{-1}$, and 15.0 $°C \cdot min^{-1}$ from ambient temperature to 500 °C. The temperature and heat were calibrated using pure indium and tin particles. The DSC and TG-DTG curves obtained under the same conditions overlap with each other, indicating that the reproducibility of tests was satisfactory.

RESULTS AND DISCUSSION

Crystal structure. The selected bond lengths, bond angles, and hydrogen bonds are listed in Tables 2 and 3. The molecular structure, one-dimensional chain, three-dimension structure, and crystal packing are illustrated in Figs. 1—4 respectively.

The analytical results indicate that within each molecule there is a non-crystallographic twofold axis (Fig. 1). The atoms on the four-membered ring are nearly in a plane. Carbonyls with the four-membered ring are almost coplanar. The dihedral angle between two azetidine rings is 6.5°. The gem-dinitro groups are mutually perpendicular. From the experimental results on bond lengths in Table 1, the C(2)—N(2) bond length is 1.519 Å, longer than that of the conventional C—N bond (1.47—1.50 Å)

Table 2

Selected bond lengths (Å) *and bond angles* (deg.) *of* $(DNAZ\text{-}CO)_2$

Bonds	Expt	Calcd.	Bonds	Expt	Calcd.	Bonds	Expt	Calcd.
C(1)—C(2)	1.518(4)	1.545	N(3)—O(3)	1.211(4)	1.224	C(4A)—C(4)—O(5)	121.9(3)	123.1
C(1)—N(1)	1.459(4)	1.470	N(3)—O(4)	1.199(4)	1.238	N(1)—C(4)—O(5)	123.3(3)	122.7
C(2)—C(3)	1.531(5)	1.551	C(2)—C(1)—N(1)	87.4(2)	87.7	C(1)—N(1)—C(3)	95.5(2)	101.2
C(2)—N(2)	1.519(5)	1.544	C(1)—C(2)—C(3)	90.3(3)	89.5	C(1)—N(1)—C(4)	128.0(3)	127.3
C(2)—N(3)	1.497(5)	1.533	C(1)—C(2)—N(2)	114.8(3)	114.7	C(3)—N(1)—C(4)	135.8(3)	137.1
C(3)—N(1)	1.461(4)	1.477	C(1)—C(2)—N(3)	117.2(3)	115.5	C(2)—N(2)—O(1)	116.1(3)	115.2
C(4)—N(1)	1.320(4)	1.353	C(3)—C(2)—N(2)	115.9(3)	116.4	C(2)—N(2)—O(2)	117.6(3)	117.5
C(4)—C(4A) #1	1.521(5)	1.539	C(3)—C(2)—N(3)	113.2(2)	113.3	O(1)—N(2)—O(2)	126.3(4)	127.4
C(4)—O(5)	1.223(3)	1.239	N(2)—C(2)—N(3)	105.5(3)	107.1	C(2)—N(3)—O(3)	117.9(4)	117.6
N(2)—O(1)	1.193(4)	1.232	C(2)—C(3)—N(1)	86.8(2)	87.3	C(2)—N(3)—O(4)	116.9(3)	114.9
N(2)—O(2)	1.218(4)	1.232	C(4A)—C(4)—N(1)	114.8(3)	114.3	O(3)—N(3)—O(4)	125.1(4)	127.4

Symmetry codes: #1: *–x*, 1*–y*, *z*.

Table 3

Observed hydrogen bonds (Å, deg.) *of* $(DNAZ\text{-}CO)_2$

D—H···A	*d*(D—H)	*d*(H···A)	*d*(D···A)	∠DHA
C(3)—H(3A)#2···O(3)	0.97	2.41	3.253(6)	145.1
C(3)—H(3B)···O(5) #3	0.97	2.41	3.316(5)	155.8
C(1)—H(1A)···O(5) #4	0.97	2.41	3.376(5)	171.4

Symmetry codes: #2: 1/4+*x*, 5/4–*y*, 1/4+*z*; #3: 1/4–*x*, 1/4+*y*, 1/4+*z*; #4: 1/4+*x*, 3/4–*y*, –1/4+*z*.

[21], which indicates that the initial decomposition step of $(DNAZ\text{-}CO)_2$ is the loss of NO_2 from C(2). In fact, most of the experimental and theoretical investigations have indicated that the initial decomposition step of TNAZ is the loss of NO_2 from nitro or nitramine groups [22]. The C(4)—N(1) bond length is 1.320 Å, shorter than that of the conventional C—N bond, which should be a consequence of the carbonyl-conjugate of C(4)—N(1).

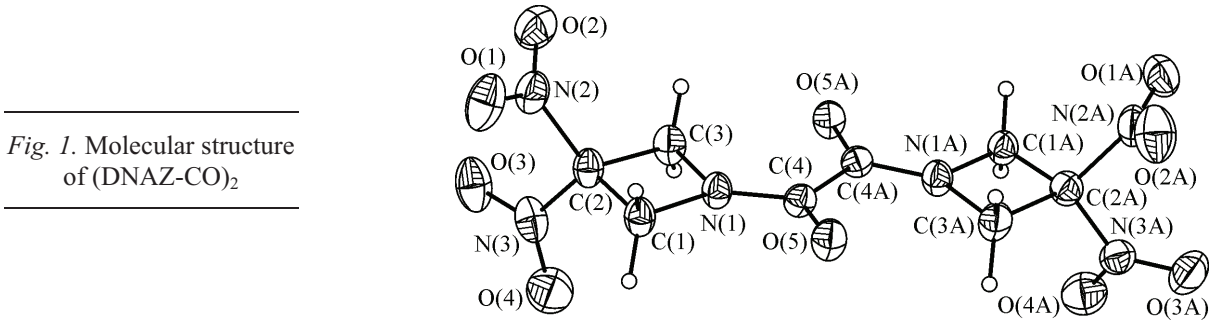

Fig. 1. Molecular structure of $(DNAZ\text{-}CO)_2$

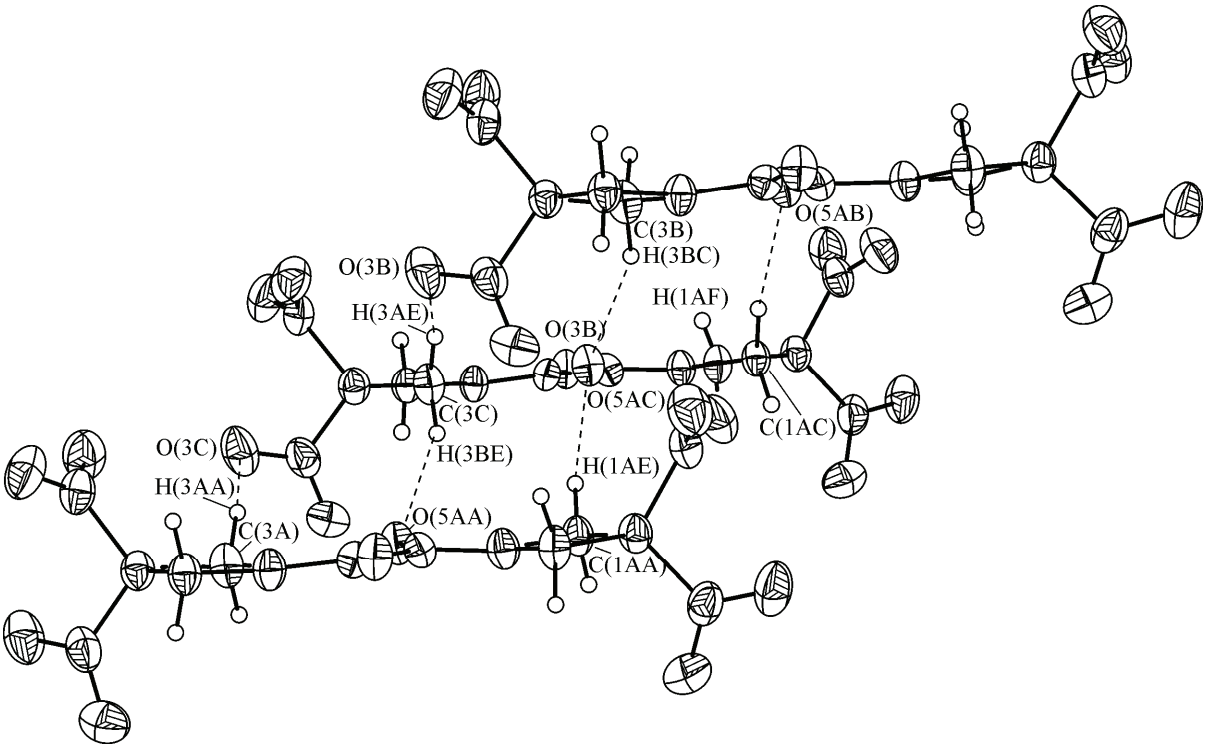

Fig. 2. One-dimensional structure of $(DNAZ\text{-}CO)_2$

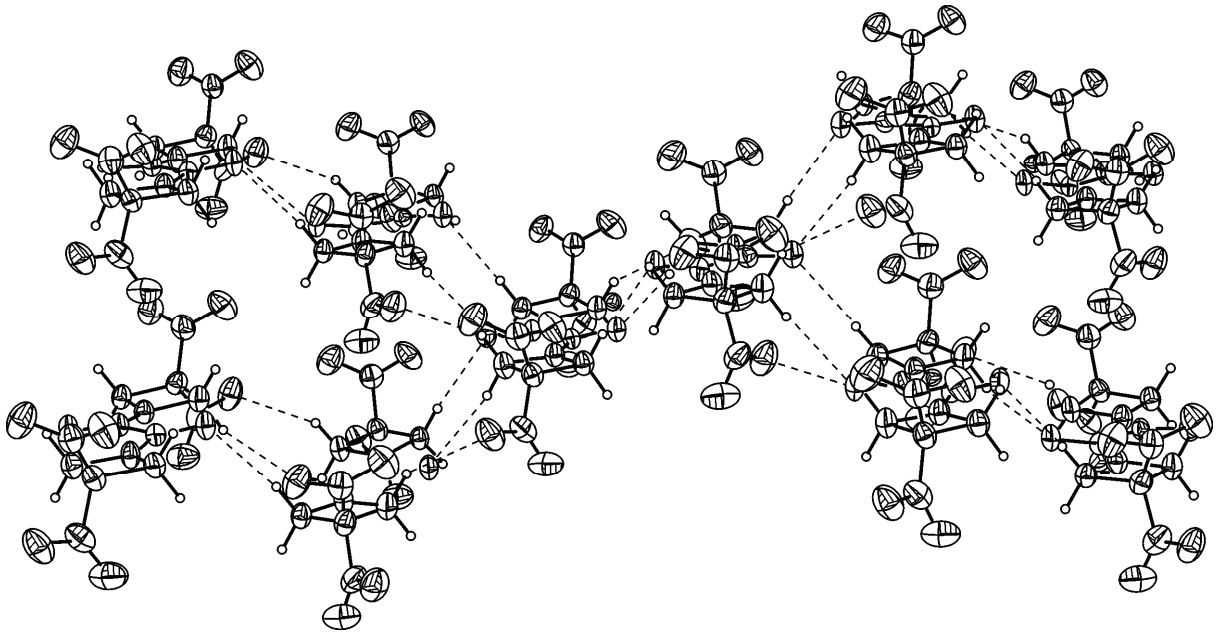

Fig. 3. Two-dimensional structure of $(DNAZ\text{-}CO)_2$

From Fig. 2, one can see that three hydrogen bonds of C(1A)—H(1AA)···O(5A), C(3)—H(3A)··· ···O(3) and C(3)—H(3B)···O(5A) form a one-dimensional chain. There is a non-crystallographic twofold axis in each molecule, which makes the same hydrogen bonds C(1)—H(1A)···O(5), C(3A)—H(3AA)···O(3A) and C(3A)—H(3AB)···O(5) form a three-dimension structure (Fig. 3).

Frontier orbital energy and orbital percentage. The frequency calculation shows no imaginary frequency, which indicates that our optimized geometry is the stable one. Table 2 lists the calculated bond lengths and bond angles. The calculated values are nearly in agreement with experimental ones. The largest deviation (0.039 Å, 5.7°) and the root mean squared errors (0.025 Å, 1.6°) for the bond lengths and angles were calculated, which indicates that the optimized geometry is objective and credible.

There is a non-crystallographic twofold axis in the molecule, so its molecular orbital is symmetrical; this state of the molecular orbital is labeled A and B in ADF. There are 89 occupied molecular orbitals according to the selected basic set and molecular structure, leading to that the number of A-type orbitals exceeds by one the number of B-type occupied orbitals, so the highest occupied molecular orbital (HOMO) is A-type. The results show that the lowest unoccupied molecular orbital (LUMO) energy of A-type and B-type is exactly the same, so LUMO is of two types; they are composed of identical atoms with a little different percentage (Table 4). HOMO is mainly composed of

Table 4

Frontier orbital energy (eV) *data and orbital percentage* (%) *in* HOMO *and* LUMO *for* $(DNAZ\text{-}CO)_2$

E_{HOMO}	E_{LUMO}	$\Delta E_{L—H}$*	Main atomic orbital percentage in HOMO and LUMO (%)	
			HOMO	LUMO(A/B)
–6.639	–4.336	2.303	C(4):8.70	N(2):31.91/29.59 N(3):5.68/8.18
			N(1):4.96	O(1):26.06/24.34 O(2):26.42/24.46
			O(5):79.53	O(3):3.70/5.84 O(4):3.66/5.73

* $\Delta E_{L—H} = E_{LUMO} - E_{HOMO}$.

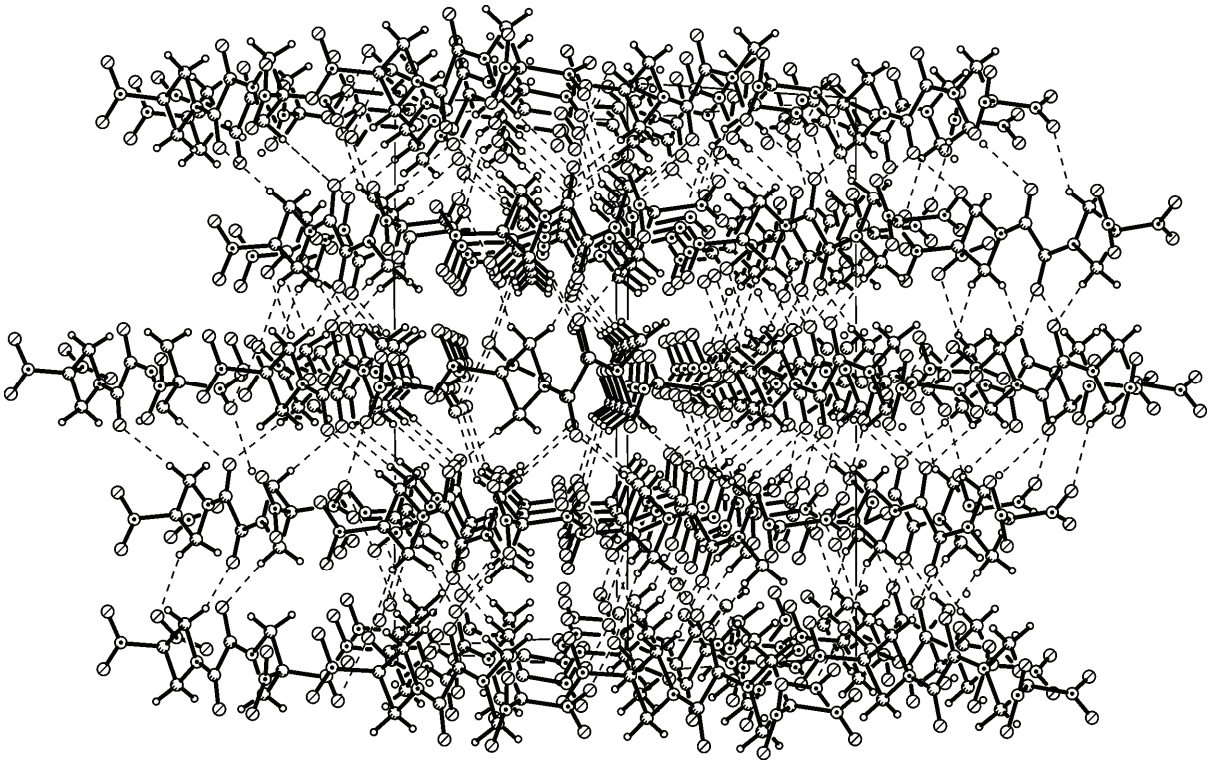

Fig. 4. Packing diagram of $(DNAZ\text{-}CO)_2$

oxygen of carbonyl indicating that O(5) of carbonyl is the point of molecular reactivity; LUMO is mainly composed of nitro N(2)O(1)O(2). The $\Delta E_{L—H}$ of $(DNAZ\text{-}CO)_2$ is larger than *N*-acetyl-3,3-dinitroazetidine (ADNAZ, 2.09 eV), and *N*-formyl-3,3-dinitroazetidine (FDNAZ, 2.08 eV) [9], which indicates that $(DNAZ\text{-}CO)_2$ is more stable than ADNAZ and FDNAZ.

Thermal behavior. Typical DSC and TG-DTG curves for $(DNAZ\text{-}CO)_2$ are shown in Figs. 5 and 6. The DSC curve indicates that the thermal decomposition of $(DNAZ\text{-}CO)_2$ is composed of one exothermic process with a peak temperature of 283.21 °C. The TG-DTG curves also show one stage of the mass loss process, which begins at about 165.81 °C and completes at 450.03 °C with a mass loss of 90.18 %.

In order to obtain the kinetic parameters (apparent activation energy (E_a), pre-exponential factor (A), and linear correlation coefficient (r)) of the main exothermic decomposition reaction for (DNAZ-

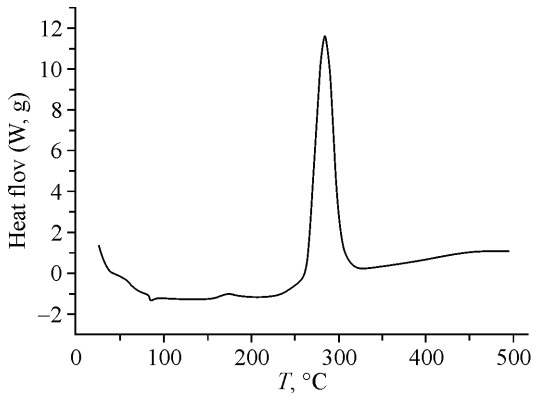

Fig. 5. DSC curve of $(DNAZ\text{-}CO)_2$ at 10 °C·min^{-1}

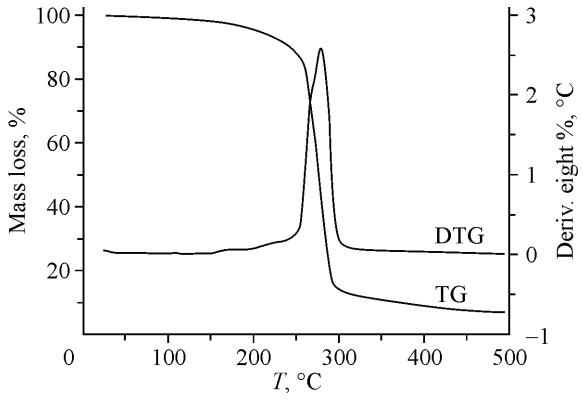

Fig. 6. TG/DTG curve of $(DNAZ\text{-}CO)_2$ at 10 °C·min^{-1}

Table 5

Calculated values of the kinetic parameters for the exothermic decomposition reaction of $(DNAZ\text{-}CO)_2$ *determined from the DSC curves at various heating rates*

β, °C·min^{-1})	T_p, °C	E_k, kJ·mol^{-1}	log, A_k/s^{-1}	r_k	E_o, kJ·mol^{-1}	r_o
2.5	264.97	163.76	13.38	0.9949	164.44	0.9955
5.0	272.70					
10.0	283.21					
15.0	291.00					

Mean: $E = (163.76 + 164.44)/2 = 164.10$ kJ·mol^{-1}

B is the heating rate; T_p is the maximum peak temperature; *E* is the apparent activation energy; *A* is the pre-exponential constant; *r* is the linear correlation coefficient; subscript *k* denotes the data obtained by Kissinger′s method; subscript o means the data obtained by Ozawa′s method.

$CO)_2$, two model-free isoconversional methods [Eqs. (1)—(2)] were employed. These methods are as follows: the Kissinger equation [23]

$$\ln\frac{\beta}{T_p^2} = \ln\frac{AR}{E_a} - \frac{E_a}{RT_p} \tag{1}$$

and the Flynn—Wall—Ozawa (F-W-O) equation [24]

$$\lg\beta + \frac{0.4567E_\alpha}{RT} = C, \tag{2}$$

where *T* is the absolute temperature, E_α is the apparent activation energy, β is the heating rate, *R* is the gas constant, T_p is the peak temperature of the DSC curve, and *A* is the pre-exponential factor.

The calculated values are listed in Table 5. The apparent activation energy and the pre-exponential factor of the exothermic decomposition reaction are 164.10 kJ·mol^{-1} and $10^{13.38}$ s^{-1} respectively.

The value (T_{po}) of the peak temperature (T_p) corresponding to $\beta \to 0$ obtained by Eq. (3) taken from [25] is 257.19 °C.

$$T_p = T_{po} + a\beta_i + b\beta_i^2 + c\beta_i^3 i = 1-4, \tag{3}$$

where *a*, *b*, and *c* are coefficients.

The corresponding critical temperature of thermal explosion (T_{bp}) obtained from Eq. (4) taken from [26] is 272.20 °C.

$$T_{bp} = \frac{E_o - \sqrt{E_o^2 - 4E_oRT_{po}}}{2R}. \tag{4}$$

The entropy of activation ($\Delta S^{\neq}$), enthalpy of activation ($\Delta H^{\neq}$), and Gibbs free energy of activation ($\Delta G^{\neq}$) corresponding to $T = T_{po}$, $E_a = E_k$ and $A = A_k$ obtained by Eqs. (5)—(7) are 6.44 J·mol^{-1}·K^{-1}, 163.76 kJ·mol^{-1}, and 160.34 kJ·mol^{-1}respectively.

$$A = \frac{k_B T}{h} e^{\Delta S^{\neq}/R}. \tag{5}$$

$$A\exp(-E_a / RT) = \frac{k_B T}{h}\exp\left(\frac{\Delta S^{\neq}}{R}\right)\exp\left(-\frac{\Delta H^{\neq}}{RT}\right). \tag{6}$$

$$\Delta G^{\neq} = \Delta H^{\neq} - T\Delta S^{\neq}, \tag{7}$$

where k_B is the Boltzmann constant and *h* is the Plank constant.

CONCLUSIONS

The analytical results of the crystal structure study indicate that the initial decomposition step of $(DNAZ\text{-}CO)_2$ is the loss of NO_2 from C(2). The O(5) atom of carbonyl is the point of molecular reactivity and $(DNAZ\text{-}CO)_2$ is more stable than ADNAZ and FDNAZ, according to the quantum chemical calculations. The apparent activation energy and pre-exponential factor of the exothermic thermal decomposition reaction are 164.10 $kJ \cdot mol^{-1}$ and $10^{13.38}$ s^{-1} respectively. The critical temperature of thermal explosion is 272.20 °C. The $\Delta S^{\neq}$, $\Delta H^{\neq}$, and $\Delta G^{\neq}$ values of this reaction are 6.44 $J \cdot mol^{-1} \cdot K^{-1}$, 163.76 $kJ \cdot mol^{-1}$, and 160.34 $kJ \cdot mol^{-1}$ respectively.

Acknowledgments. This work is supported by the National Natural Science Foundation of China (Grant Nos.20603026 and 21073141), the Provincial Natural Foundation of Shaanxi (Grant No. 2009JQ2002), NWU Graduate Experimental Research Funds (Grant No. 09YSY23), and the Project sponsored by SRF for AT, YLU (Grant No. 09GK019).

REFERENCES

1. *Archibald T.G., Gilardi R., Baum K. et al.* // J. Org. Chem. – 1990. – **55**. – P. 2920.
2. *Hiskey M.A., Coburn M.D., Mitchell M.A. et al.* // J. Heterocyclic. Chem. – 1992. – **29**. – P. 1855.
3. *Hiskey M.A., Stincipher M.M., Brown J.E.* // J. Energ. Mater. – 1993. – **11**. – P. 157.
4. *Dejaegher Y., Kuz'menok N.M., Zvonok A.M. et al.* // Chem. Rev. – 2002. – **102**. – P. 29.
5. *Ma H.X., Yan B., Li J.F. et al.* // J. Mol. Struct. – 2010. – **981**. – P. 103.
6. *Ma H.X., Yan B., Li Z.N. et al.* // J. Therm. Anal. Calorim. – 2009. – **95**. – P. 437.
7. *Ma H.X., Yan B., Li Z.N. et al.* // J. Hazard. Mater. – 2009. – **169**. – P. 1068.
8. *Li Z.N., Ma H.X., Yan B. et al.* // Chinese. J. Chem. – 2009. – **27**. – P. 2284.
9. *Ma H.X., Yan B., Song J.R. et al.* // Chem. J. Chinese. U. – 2009. – **30**. – P. 377 (in Chinese).
10. *Gao R., Ma H.X., Yan B. et al.* // Chem. J. Chinese. U. – 2009. – **30**. – P. 577 (in Chinese).
11. *Yan B., Ma H.X., Hu Y. et al.* // Acta Crystallogr. – 2009. – **E65**. – P. o3215.
12. *Yan B., Ma H.X., Li J.F. et al.* // Acta Crystallogr. – 2010. – **E66**. – P. o57.
13. *te Velde G., Bickelhaupt F.M., Baerends E.J. et al.* // J. Comput. Chem. – 2001. – **22**. – P. 931.
14. *Fonseca Guerra C., Snijders J.G., te Velde G. et al.* // Theor. Chem. Acc. – 1998. – **99**. – P. 391.
15. *Baerends E.J., Autschbach J., Bérces A. et al.* // ADF2005.01, SCM, Theoretical Chemistry, Vrije Universiteit, Amsterdam, The Netherlands, 2005.
16. *Sheldrick G.M.* SADABS, Siemens area detector absorption corrected software, University of Göttingen, Göttingen, Germany, 2000.
17. *Sheldrick G.M.* SHELXTL-97, Program for crystal structures refinement, University of Göttingen, Göttingen, Germany, 1997.
18. *Vosko S.H., Wilk L., Nusair M.* // Can. J. Phys. – 1980. – **58**. – P. 1200.
19. *Adamo C., Barone V.* // J. Chem. Phys. – 1998. – **108**. – P. 664.
20. *Perdew J.P., Chevary J.A., Vosko S.H. et al.* // Phys. Rev. B. – 1992. – **46**. – P. 6671.
21. *Harmony M.D., Laurie V.W., Kuczkowski R.L. et al.* // J. Phys. Chem. Ref. Data. – 1979. – **8**. – P. 619.
22. *Zhao Q.H., Zhang S.W., Li Q.S.* // Chem. Phy. Let. – 2005. – **412**. – P. 317.
23. *Kissinger H.E.* // Anal. Chem. – 1957. – **29**. – P. 1702.
24. *Ozawa T.* // Chem. Soc. Jpn. – 1965. – **38**. – P. 1881.
25. *Hu R.Z., Yang Z.Q., Liang Y.J.* // Thermochim. Acta. – 1988. – **123**. – P. 135.
26. *Zhang T.L., Hu R.Z., Xie Y. et al.* // Thermochim. Acta. – 1994. – **244**. – P. 171.